

# Non-perturbative Renormalization Group of a $U(1)$ Tensor Model



Vincent Lahoche and Dine Ousmane Samary

*To Professor Mahouton Norbert Hounkonnou*

**Abstract** This paper aims at giving some comment on our new development on the functional renormalization group applied to the  $U(1)$  tensor model previously studied in [Phys. Rev. D 95, 045013 (2017)]. Using the Wetterich non-perturbative equation, the flow of the couplings and mass parameter are discussed and the physical implication such as the asymptotically safety of the model is provided.

**Keywords** Random tensor models · Functional renormalization group · Flow equation

## 1 Introduction

Random Tensor Models [1–3] extends Matrix Models as promising candidates to understand Quantum Gravity in higher dimension,  $D \geq 3$ . Especially colored tensor models allow one to define probability measures on simplicial pseudo-manifolds, and they are considered as a convenient formalism for studying random geometries [3–8]. On the other hand, group field theory aims at describing a rudimentary phase of the geometry of spacetime, namely when this geometry is hypothetically still in a discrete form, or at least not yet continuous (the geometrogenesis scenario)

---

V. Lahoche

LaBRI, Univ. Bordeaux 351 cours de la Libération, Talence, France

e-mail: [vincent.lahoche@labri.fr](mailto:vincent.lahoche@labri.fr)

D. Ousmane Samary (✉)

Max Planck Institute for Gravitational Physics, Albert Einstein Institute, Potsdam, Germany

Faculté des Sciences et Techniques/ICMPA-UNESCO Chair, Université d'Abomey-Calavi, Abomey-Calavi, Benin

e-mail: [dine.ousmanesamary@aei.mpg.de](mailto:dine.ousmanesamary@aei.mpg.de)

© Springer Nature Switzerland AG 2018

T. Diagana, B. Toni (eds.), *Mathematical Structures and Applications*,

STEAM-H: Science, Technology, Engineering, Agriculture,

Mathematics & Health, [https://doi.org/10.1007/978-3-319-97175-9\\_13](https://doi.org/10.1007/978-3-319-97175-9_13)

[9–12]. It is also named “pre-geometric” phase of our spacetime. Recently Tensor models and group field theory have been combined to provide a new class of field theories so-called tensorial group field theory (TGFT). TGFTs improve the group field theories in order to allow for renormalization [13–17]. Moreover, it has been shown that several TGFT models are asymptotically free in the UV, in other words, near the Gaussian fixed point [17–26].

Much interest was focused on the FRG equation of various Matrix and TGFT models [20–29]. The flow equations also called the Wetterich equations were derived [30]. The fixed points were given and further evidence of asymptotically safety and asymptotically freedom were derived around these fixed points in the UV. The TGFT of the form  $T_5^6$  on the  $U(1)$  group with closure constraint is proved to be renormalizable [15]. The proof of this claim is performed using multi-scale analysis. The closure constraint also called gauge invariance condition can help to define the emergence of the metric on spacetime after phase transition and therefore makes this type of model relevant for the understanding the quantum theory of gravitation. This kind of model with closure constraint, namely the six-dimensional TGFT with quartic interactions is studied recently in [20] and [22]. The perturbative computation of the  $\beta$ -functions of the  $T_5^6$  model is given in [19], in which we have showed that this model is asymptotically free in the UV. This result seems to be nonconsistent from the point of view of the FRG analysis. This work aims at giving our new contributions on the  $U(1)$  TGFT such as the renormalization theorems and the functional renormalization group analysis to show the asymptotically safety of these type of models.

Our paper is organized as follows. Section 2 is devoted to present the model which is analyzed in this work, namely the  $T_5^6$  model with closure constraints. In Sect. 3 the flow equations of the coupling constants and mass parameter are derived by using the dimensional renormalization parameters. In Sect. 4 we give the nontrivial fixed points and provide the numerical solution of the flow equations. The behavior of the model we studied in the vicinity of these fixed points is also given. The conclusion is made in Sect. 5.

## 2 $U(1)^d$ Tensorial Group Field Theory

In this section we give some basic notations and definitions of the TGFT that have been used in this note. Particularly we will use a power counting theorem to discuss the notion of canonical dimensions for each coupling. The canonical dimension allows us to make sense of the exponentiation of the action in the partition function.

We start by defining an action  $S[\bar{\varphi}, \varphi]$  of TGFT that depends on the field  $\varphi$  and its conjugate  $\bar{\varphi}$  acting on the compact Lie group  $G$ , i.e.,

$$\varphi : G^d \longrightarrow \mathbb{C}; \quad (g_1, \dots, g_d) \longmapsto \varphi(g_1, \dots, g_d). \quad (2.1)$$

We will always consider  $G = U(1)$ , but the analysis performed here can be extended to over groups. We are using the Fourier transformation of the field and are defining the momentum variable associated with the group elements  $\vec{g} = (g_1, g_2, \dots, g_d) \in U(1)^d$  as  $\vec{p} = (p_1, p_2, \dots, p_d) \in \mathbb{Z}^d$ . Using the parametrization  $g_k = e^{i\theta_k}$  we write

$$\varphi(g_1, \dots, g_d) = \sum_{p_i \in \mathbb{Z}} \varphi(p_1, \dots, p_d) e^{i \sum_k \theta_k p_k}, \quad \theta_i \in [0, 2\pi), \quad (2.2)$$

where we denote the Fourier transform of the field  $\varphi$  by  $\varphi_{12\dots d} =: \varphi(p_1, \dots, p_d) =: \varphi_{\vec{p}}$  for simplicity. The functional action  $S[\bar{\varphi}, \varphi]$  is written in general case as

$$S[\bar{\varphi}, \varphi] = \sum_{p_i} \bar{\varphi}_{\vec{p}} C^{-1}(\vec{p}, \vec{p}') \varphi_{\vec{p}} \prod_{i=1}^D \delta_{p_i p'_i} + S_{\text{int}}[\bar{\varphi}, \varphi] \quad (2.3)$$

where  $C$  stands for the propagator and  $S_{\text{int}}$  collects all vertex contributions of the interaction.

Let  $d\mu_C$  be the field measure associated with the covariance  $C$ , we have the relation

$$C(\vec{p}, \vec{p}') = \int d\mu_C \varphi_{\vec{p}} \bar{\varphi}_{\vec{p}'}, \quad d\mu_C = \prod_{\vec{p}} d\bar{\varphi}_{\vec{p}} d\varphi_{\vec{p}} e^{-\bar{\varphi}_{\vec{p}} C^{-1}(\vec{p}, \vec{p}') \varphi_{\vec{p}}}. \quad (2.4)$$

We introduce a cut-off  $\Lambda$  on  $C_{\vec{p}, \vec{p}'}$ , impose that to satisfy  $|\vec{p}| \leq \Lambda$ . The generating function or the vacuum–vacuum transition amplitude is

$$Z_\Lambda[J, \bar{J}] = e^{W_\Lambda[J, \bar{J}]} = \int d\mu_{C_\Lambda}(\bar{\varphi}, \varphi) e^{S_{\text{int}}[\bar{\varphi}, \varphi] + \langle \bar{J}, \varphi \rangle + \langle \bar{\varphi}, J \rangle} \quad (2.5)$$

where the notation  $\langle ., . \rangle$  means:  $\langle \bar{J}, \varphi \rangle = \sum_{\vec{p} \in \mathbb{Z}^d} \bar{J}_{\vec{p}} \varphi_{\vec{p}}$ ,  $d\mu_{C_\Lambda}$  is the Gaussian measure with the covariance  $C_\Lambda$  such that:

$$\int d\mu_{C_\Lambda} \varphi_{\vec{p}} \bar{\varphi}_{\vec{p}'} = \frac{e^{-(\vec{p}^2 + m^2)/\Lambda^2}}{\vec{p}^2 + m^2} \delta\left(\sum_{i=1}^d p_i\right) \delta_{\vec{p}\vec{p}'} = C_\Lambda(\vec{p}, \vec{p}') \quad (2.6)$$

and the delta  $\delta(\sum_{i=1}^d p_i)$  implements the closure constraint, see [13]. We keep in mind that we must send the cut-off to infinity in any circumstances. We define a model by its action at a high (UV) energy scale. The classical action  $S_{\text{int}}$  is defined as a sum of tensorial invariants [3]:

$$S_{\text{int}}[\bar{\varphi}, \varphi] = \sum_{b \in \mathcal{B}} \lambda_b \text{Tr}_b[\bar{\varphi}, \varphi]. \quad (2.7)$$

A tensor invariant is a polynomial in the tensor  $\varphi$  and its conjugate  $\bar{\varphi}$  which is invariant under the action of the tensor product of  $d$  independent copies of the unitary group  $U(N)$ . The sum is taken over a finite set  $\mathcal{B}$  of such invariants  $d$ -bubbles [3] associated with the couplings  $\lambda_b$ . The interaction (2.7) of a tensor field theory in dimension  $d = 5$  [15] is

$$\begin{aligned}
 S_{int}[\bar{\varphi}, \varphi] = & \frac{\lambda_1}{2} \sum_{\ell=1}^5 \sum_{\vec{p}_i} \mathcal{W}_{\vec{p}_1, \vec{p}_2, \vec{p}_3, \vec{p}_4}^{(\ell)} \varphi_{\vec{p}_1} \bar{\varphi}_{\vec{p}_2} \varphi_{\vec{p}_3} \bar{\varphi}_{\vec{p}_4} \\
 & + \frac{\lambda_2}{3} \sum_{\ell=1}^5 \sum_{\vec{p}_i} \mathcal{X}_{\vec{p}_1, \vec{p}_2, \vec{p}_3, \vec{p}_4, \vec{p}_5, \vec{p}_6}^{(\ell)} \varphi_{\vec{p}_1} \bar{\varphi}_{\vec{p}_2} \varphi_{\vec{p}_3} \bar{\varphi}_{\vec{p}_4} \varphi_{\vec{p}_5} \bar{\varphi}_{\vec{p}_6} \\
 & + \lambda_3 \sum_{\ell_i=1, i=1,2,3}^5 \sum_{\vec{p}_i} \mathcal{Y}_{\vec{p}_1, \vec{p}_2, \vec{p}_3, \vec{p}_4, \vec{p}_5, \vec{p}_6}^{(\ell_1, \ell_2, \ell_3)} \varphi_{\vec{p}_1} \bar{\varphi}_{\vec{p}_2} \varphi_{\vec{p}_3} \bar{\varphi}_{\vec{p}_4} \varphi_{\vec{p}_5} \bar{\varphi}_{\vec{p}_6}, \quad (2.8)
 \end{aligned}$$

where the symbols  $\mathcal{W}^{(\ell)}$ ,  $\mathcal{X}^{(\ell)}$ , and  $\mathcal{Y}^{(\ell)}$  are products of delta functions associated with tensor invariant interactions, and  $\lambda_i(\Lambda)$  are coupling constants. For instance:

$$\mathcal{W}_{\vec{p}_1, \vec{p}_2, \vec{p}_3, \vec{p}_4}^{(\ell)} = \delta_{p_{1\ell} p_{4\ell}} \delta_{p_{2\ell} p_{3\ell}} \prod_{j \neq \ell} \delta_{p_{1j} p_{2j}} \delta_{p_{3j} p_{4j}}. \quad (2.9)$$

Such a kernel is called *bubble* [3], and can be pictured graphically as a 6-colored bipartite regular graph, with black and white vertices corresponding, respectively, to the fields  $\varphi$  and  $\bar{\varphi}$ , and each line corresponding to a Kronecker delta.

$$\begin{aligned}
 \mathcal{W}^{(\ell)}(\mathbf{g}_1, \mathbf{g}_2, \mathbf{g}_3, \mathbf{g}_4) &= \text{Diagram 1} \\
 \mathcal{X}^{(\ell)}(\mathbf{g}_1, \mathbf{g}_2, \mathbf{g}_3, \mathbf{g}_4, \mathbf{g}_5, \mathbf{g}_6) &= \text{Diagram 2} \\
 \mathcal{Y}^{(\ell_1, \ell_2, \ell_3)}(\mathbf{g}_1, \mathbf{g}_2, \mathbf{g}_3, \mathbf{g}_4, \mathbf{g}_5, \mathbf{g}_6) &= \text{Diagram 3}
 \end{aligned} \quad (2.10)$$

$$\mathcal{X}^{(\ell)}(\mathbf{g}_1, \mathbf{g}_2, \mathbf{g}_3, \mathbf{g}_4, \mathbf{g}_5, \mathbf{g}_6) = \begin{array}{c} S \quad \bar{S} \\ \swarrow \quad \searrow \\ S_1 \\ \downarrow \\ S_0 \end{array} \quad (2.11)$$

$$\mathcal{Y}^{(\ell_1, \ell_2, \ell_3)}(\mathbf{g}_1, \mathbf{g}_2, \mathbf{g}_3, \mathbf{g}_4, \mathbf{g}_5, \mathbf{g}_6) = \begin{array}{c} \mathcal{L}_0 \\ \downarrow \\ \mathcal{L}_1 \\ \swarrow \quad \searrow \\ \mathcal{L} \quad \bar{\mathcal{L}} \end{array} \quad (2.12)$$

Let  $\mathcal{G}$  be a 2- or 4 or 6-point Feynman graph of model (2.8). Let be denoted by  $\omega(\mathcal{G})$  the degree of the tensor graph  $\mathcal{G}$ , i.e.:

$$\omega(\mathcal{G}) = \sum_{J \text{ jacket of } \mathcal{G}} g_J \quad (2.13)$$

where  $g_J$  is the genus of the jacket  $J$ . A simple way of computing the degree  $\omega$  of a graph is to count its number  $F$  of faces. Let us pick an arbitrary orientation for all of the edges  $e$  and for all of the faces  $f$ . Then  $R$  is the rank of the incidence matrix  $\epsilon_{fe}$ :

$$\epsilon_{fe} = \begin{cases} 1 & \text{if } e \in f \text{ and their orientation match} \\ -1 & \text{if } e \in f \text{ and their orientation do not match} \\ 0 & \text{otherwise.} \end{cases} \quad (2.14)$$

One can show that the rank  $R$  does not depend on the chosen orientation. We get the following results (see [15] for more detail):

**Proposition 2.1 (Divergence Degree)** *The degree of divergence  $\omega_d$  of a  $\varphi_d^n U(1)^d$  model is given by*

$$\omega_d(\mathcal{G}) = (-2L + F - R)(\mathcal{G}) \quad (2.15)$$

$$\begin{aligned} &= -\frac{2}{(d-1)!}(\omega(\mathcal{G}) - \omega(\partial\mathcal{G})) - (C_{\partial\mathcal{G}} - 1) - \frac{d-3}{2}N(\mathcal{G}) + (d-1) \\ &\quad + \frac{d-3}{2}nV(\mathcal{G}) - (d-1)V(\mathcal{G}) - R(\mathcal{G}) \end{aligned} \quad (2.16)$$

where  $V(\mathcal{G})$  is the number of vertices of  $\mathcal{G}$ ,  $N(\mathcal{G})$  its number of external legs, and  $C_{\partial\mathcal{G}}$  is the number of connected components of its boundary graph  $\partial\mathcal{G}$  and  $\tilde{\omega}(\mathcal{G}) = \sum_{\tilde{J} \subset \mathcal{G}} g_{\tilde{J}}$  with  $\tilde{J}$  the pinched jacket associated with a jacket  $J$  of  $\mathcal{G}$ ,  $C_{\partial\mathcal{G}}$  is the number of vertex-connected components of  $\partial\mathcal{G}$ .

**Lemma 2.2** *Let  $\mathcal{G}$  be a connected Feynman graph and  $\mathcal{T}$  one of its spanning trees. If the rosette  $\mathcal{G}/\mathcal{T}$  is fully melonic and*

**Table 1** Classification of divergent graphs

$N$	$\tilde{\omega}(\mathcal{G})$	$\omega(\partial\mathcal{G})$	$C_{\partial\mathcal{G}} - 1$	$\omega_d(\mathcal{G})$
2	0	0	0	2
4	0	0	0	1
4	0	0	1	0
6	0	0	0	0

$$F(\mathcal{G}) = (d - 1)(L(\mathcal{G}) - V(\mathcal{G}) + 1), \tag{2.17a}$$

$$R(\mathcal{G}) = R_m(\mathcal{G}) = L(\mathcal{G}) - V(\mathcal{G}) + 1, \tag{2.17b}$$

$$2\omega_d(\mathcal{G}) = - (d - 4)N(\mathcal{G}) + (d - 4)nV(\mathcal{G}) - 2(d - 2)V(\mathcal{G}) + 2(d - 2). \tag{2.17c}$$

**Proposition 2.3** *The divergent graphs of the models are classified in Table 1.*

Another important definition for our purpose concerns the notion of *canonical dimension*. We will only give the essential here, and the reader interested in the details may consult [22]. In our model, the divergence degree for an arbitrary Feynman graph  $\mathcal{G}$  is given in proposition (2.1) Denoting by  $n_i(\mathcal{G})$  the number of bubbles in  $\mathcal{G}$  with  $2i$  black and white nodes, the divergent sub- graphs are said to be melonic [7, 13], if and only if they satisfy the following relation:

$$F(\mathcal{G}) - R(\mathcal{G}) = 3(L(\mathcal{G}) - \sum_i n_i(\mathcal{G}) + 1) \tag{2.18}$$

which together with the topological relation  $L(\mathcal{G}) = \sum_i i n_i(\mathcal{G}) - N(\mathcal{G})/2$  leads to:

$$\omega_d(\mathcal{G}) = 3 - \frac{N(\mathcal{G})}{2} - 2n_1(\mathcal{G}) - n_2(\mathcal{G}), \tag{2.19}$$

where  $N(\mathcal{G})$  denote the number of external lines of  $\mathcal{G}$ . For the rest  $n_1(\mathcal{G}) = 0$ . For  $N = 4$ ,  $\omega \leq 1$ , the value 1 corresponding to melonic graphs with only 6-point interactions bubble. This conclusion indicates that perturbatively around the Gaussian Fixed Point (GFP), the coupling constant  $\lambda_1$  scales as  $\Lambda$  for some cut-off  $\Lambda$ , and we associate a canonical dimension  $[\lambda_1] = 1$  to this constant. In the same way, we deduce that for a generic coupling  $\lambda_b$ , associated to a melonic bubble with  $N_b$  external lines:

$$[\lambda_b] = 3 - \frac{N_b}{2} \tag{2.20}$$

giving explicitly:

$$[m] = 1 \quad [\lambda_1] = 1 \quad [\lambda_2] = [\lambda_3] = 0. \tag{2.21}$$

### 3 Functional Renormalization Group with Closure Constraint

The FRG method is based on the following deformation to our original partition function given in Eq. (2.5), i.e.,

$$Z_s[J, \bar{J}] = \int d\mu_{C_\Lambda}(\bar{T}, T) e^{S_{int}[\bar{T}, T] - \Delta S_s[\bar{T}, T] + \langle \bar{J}, T \rangle + \langle \bar{T}, J \rangle} \quad (3.1)$$

where  $T_{\vec{p}}$  denotes the mean field  $T_{\vec{p}} := \frac{\partial \log Z_s}{\partial J_{\vec{p}}}$ , and is a gauge invariant field in the sense that:  $T_{\vec{p}} = T_{\vec{p}} \delta(\sum_{i=1}^5 p_i)$ , and we have added to the original action an IR cut-off  $\Delta S_s[\bar{T}, T]$ , defined as:

$$\Delta S_s[\bar{T}, T] = \sum_{\vec{p} \in \mathbb{Z}^5} R_s(|\vec{p}|) \bar{T}_{\vec{p}} T_{\vec{p}}. \quad (3.2)$$

The cut-off function  $R_s$  depends on the real parameter  $s$  playing the role of a running cut-off, and is chosen such that:

- $R_s(\vec{p}) \geq 0$  for all  $\vec{p} \in \mathbb{Z}^d$  and  $s \in (-\infty, +\infty)$ .
- $\lim_{s \rightarrow -\infty} R_s(\vec{p}) = 0$ , implying:  $\mathcal{Z}_{s=-\infty}[\bar{J}, J] = \mathcal{Z}[\bar{J}, J]$ . This condition ensures that the original model is in the family (3.1). Physically, it means that the original model is recovered when all the fluctuations are integrated out.
- $\lim_{s \rightarrow \ln \Lambda} R_s(\vec{p}) = +\infty$ , ensuring that all the fluctuations are frozen when  $e^s = \Lambda$ . As a consequence, the bare action will be represented by the initial condition for the flow at  $s = \ln \Lambda$ .
- For  $-\infty < s < \ln \Lambda$ , the cut-off  $R_s$  is chosen so that  $R_s(|p| > e^s) \ll 1$ , a condition ensuring that the UV modes  $|p| > e^s$  are almost unaffected by the additional cut-off term, while  $R_s(|p| < e^s) \sim 1$ , or  $R_s(|p| < e^s) \gg 1$ , will guarantee that the IR modes  $|p| < e^s$  are decoupled.
- $\frac{d}{ds} R_s(\vec{p}) \leq 0$ , for all  $\vec{p} \in \mathbb{Z}^d$  and  $s \in (-\infty, +\infty)$ , which means that high modes should not be suppressed more than low modes.

The equation describing the flow of the couplings, the so-called Wetterich equation has been established in [30] in the case of a theory with closure constraint: For a given cut-off  $R_s$ , the effective average action satisfies the following first order partial differential equation:

$$\partial_s \Gamma_s = \sum_{\vec{p} \in \mathbb{Z}^5} \partial_s R_s(|\vec{p}|) \cdot [\Gamma_s^{(2)} + R_k]^{-1}(\vec{p}, \vec{p}) \delta\left(\sum_{i=1}^5 p_i\right). \quad (3.3)$$

where  $\Gamma_s$ , the effective average action and is defined as the Legendre transform of the free energy  $W_s := \ln[Z_s]$  as :

$$\Gamma_s[\bar{T}, T] + \sum_{\vec{p} \in \mathbb{Z}^5} R_s(|\vec{p}|) \bar{T}_{\vec{p}} T_{\vec{p}} := \langle \bar{J}, T \rangle + \langle \bar{T}, J \rangle - W_s[J, \bar{J}] \quad (3.4)$$

and

$$\Gamma_s^{(2)}(\vec{p}, \vec{p}') := \frac{\partial^2 \Gamma_s}{\partial T_{\vec{p}} \partial \bar{T}_{\vec{p}'}}. \quad (3.5)$$

The Wetterich flow equation is an exact differential equation which must be truncated, i.e. it must be projected to functions of few variables or even onto some finite-dimensional sub-theory space. In this section, we adopt the simplest truncation, consisting in a restriction to the essential and marginal coupling with respect to the perturbative power counting (i.e., whose canonical dimension is upper or equal to zero). As mentioned before, such a truncation makes sense as long as the anomalous dimension remains small, and a qualitative argument is the following. Let us define the anomalous dimension  $\eta := \partial_s \ln(Z)$  (see Eq. (3.9) below). In the vicinity of a fixed point,  $\eta$  can reach to a non-zero value  $\eta_*$ . As a result, the effective propagator becomes:

$$\frac{Z^{-1}}{\vec{p}^2 + (m_s^2/Z)} \approx \frac{e^{-\eta_* s}}{\vec{p}^2 + m_*^2}, \quad (3.6)$$

and then modifies the power counting (2.19), which becomes in the melonic sector (all the star-quantities refers to the non-Gaussian fixed point that we consider):

$$\begin{aligned} \omega_*(\mathcal{G}) &= -(2 + \eta_*)L(\mathcal{G}) + (F(\mathcal{G}) - R(\mathcal{G})) \\ &= 3 - \frac{N}{2}(1 - \eta_*) - 3\eta_* n_3 - (1 + 2\eta_*)n_2 - (2 + \eta_*)n_1. \end{aligned} \quad (3.7)$$

As a result, the canonical dimension (2.21) turns to be

$$[t_b]_* = 3 - \frac{N_b}{2}(1 - \eta_*) = [t_b] + \frac{N_b}{2}\eta_* \quad , \quad (3.8)$$

from which one can argue that, as long as  $\eta_* \ll 1$ , the classification in terms of relevant, irrelevant and marginal couplings remains unchanged, and the truncation around marginal couplings with respect to the perturbative power counting makes sense. Note that for more specific explanations the study of the critical exponent will help to prove whether or not the truncation given below equation should improve or not. Unlike the case of standard local field theory, each line here has several strands (the theory is non-local). The contractions in the loop of the tadpole concern only 4 strands out of 5. The last strand circulates freely, and corresponds to an external momentum. It is by developing on this external variable that we generate the contribution to the anomalous dimension  $\eta$ . Thus, the quantity  $\mathcal{W}_{\vec{p}_1, \vec{p}_2, \vec{p}_3, \vec{p}_4}^{(\ell)}$  does

not explicitly depend on the momenta. The dependence on the momenta is due to the non-locality of the interactions. Up to these considerations, our choice of truncation is the following:

$$\begin{aligned}
 \Gamma_k[\bar{T}, T] = & \sum_{\vec{p} \in \mathbb{Z}^5} \left( Z(k) \vec{p}^2 + m^2(k) \right) T_{\vec{p}} \bar{T}_{\vec{p}} + \frac{\lambda_1(k)}{2} \sum_{\ell=1}^5 \sum_{\vec{p}_i} \mathcal{W}_{\vec{p}_1, \vec{p}_2, \vec{p}_3, \vec{p}_4}^{(\ell)} T_{\vec{p}_1} \bar{T}_{\vec{p}_2} T_{\vec{p}_3} \bar{T}_{\vec{p}_4} \\
 & + \frac{\lambda_2(k)}{3} \sum_{\ell=1}^5 \sum_{\vec{p}_i} \mathcal{X}_{\vec{p}_1, \vec{p}_2, \vec{p}_3, \vec{p}_4, \vec{p}_5, \vec{p}_6}^{(\ell)} T_{\vec{p}_1} \bar{T}_{\vec{p}_2} T_{\vec{p}_3} \bar{T}_{\vec{p}_4} T_{\vec{p}_5} \bar{T}_{\vec{p}_6} \\
 & + \lambda_3(k) \sum_{\ell_i=1, i=1, 2, 3}^5 \sum_{\vec{p}_i} \mathcal{Y}_{\vec{p}_1, \vec{p}_2, \vec{p}_3, \vec{p}_4, \vec{p}_5, \vec{p}_6}^{(\ell_1, \ell_2, \ell_3)} T_{\vec{p}_1} \bar{T}_{\vec{p}_2} T_{\vec{p}_3} \bar{T}_{\vec{p}_4} T_{\vec{p}_5} \bar{T}_{\vec{p}_6}. \quad (3.9)
 \end{aligned}$$

We derive the truncated flow equations for  $m^2$ ,  $Z$ , and  $\lambda_i$  from the full Wetterich equation (3.3). We write the second derivative of  $\Gamma_k$  as:

$$\begin{aligned}
 \Gamma_k^{(2)}[\bar{T}, T](\vec{p}, \vec{p}') = & \left( -Z(k) \vec{p}^2 + m^2(k) \right) \delta \left( \sum_{i=1}^5 p_i \right) \delta_{\vec{p} \vec{p}'} \\
 & + F_{k, (1)}[\bar{T}, T]_{\vec{p}, \vec{p}'} + F_{k, (2)}[\bar{T}, T]_{\vec{p}, \vec{p}'}
 \end{aligned}$$

in such a way that all the field-dependent terms of order  $2n$  are in  $F_{k, (n)}$ . In particular,  $F_{k, (1)}$  depends on  $\lambda_1(k)$ , while  $F_{k, (2)}$  depends on  $\lambda_2(k)$  and  $\lambda_3(k)$ . For the regulator  $R_k$ , we adopt the Litim cut-off [31], in which we set  $s = e^k$ :

$$R_k(|\vec{p}|) = Z(k)(k^2 - \vec{p}^2) \Theta(k^2 - \vec{p}^2), \quad (3.10)$$

and computing the first derivative with respect to  $k$ , we find:

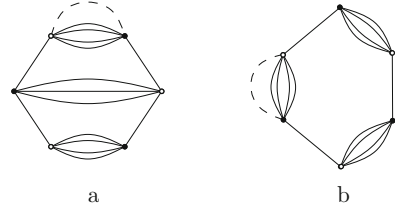
$$k \partial_k R_k(|\vec{p}|) = \{k \partial_k Z(k)(k^2 - \vec{p}^2) + 2Z(k)k^2\} \Theta(k^2 - \vec{p}^2). \quad (3.11)$$

Hence, we are now in a position to extract the flow equations for each couplings, which is the subject of the next section.

### 3.1 Flow Equations in the UV Regime

We will deduce the flow equation in the UV regime. In this regime, all the sums can be replaced by integration, following the arguments of [22], essentially because the divergences of the integral approximations are the same as the exact sums. The method consists of a formal expansion of the r.h.s of the Wetterich equation

**Fig. 1** Contributions coming from the 6-point interactions to the 4-point interaction



(3.3) in power of couplings, and an identification of the corresponding terms in the l.h.s. The r.h.s involves in general some contractions between the  $F_{k(n)}$  and the effective propagator  $\partial_k R_k$ . And in this UV regime, only the melonic graphs contribute (Fig. 1). We get the flow equation of  $m(k)$  as

$$k\partial_k m^2(k) = -\frac{4\pi}{3}\lambda_1(k)\frac{\eta(k) + 5}{[Z(k)k^2 + m^2(k)]^2}k^5 \tag{3.12}$$

with the anomalous dimension  $\eta(k)$  defined as:

$$\eta(k) := k\partial_k \ln(Z(k)) = \frac{5\pi}{2}\lambda_1(k)\frac{k^3}{[Z(k)k^2 + m^2(k)]^2 - \lambda_1(k)\frac{5}{6}\pi k^3}. \tag{3.13}$$

Note that, in this case, the extraction of the local approximation in the UV limit brings up a very nice property of the melonic sector, called *traciality*. Traciality is a concept firstly introduced in a perturbative renormalization framework, ensuring that local approximation of high subgraphs makes sense in the TFGT context [13]. The contributions to  $\lambda_1(k)$ ,  $\lambda_2(k)$ , and  $\lambda_3(k)$  are given in Figs. 2, 3 and 4 and are explicitly written as

$$k\partial_k \lambda_1(k) = -(\lambda_2(k) + 4\lambda_3(k))\frac{4\pi}{15}\frac{\eta(k) + 5}{[Z(k)k^2 + m^2(k)]^2}k^5 + \lambda_1^2(k)\frac{4\pi}{15}\frac{\eta(k) + 5}{[Z(k)k^2 + m^2(k)]^3}k^5 \tag{3.14}$$

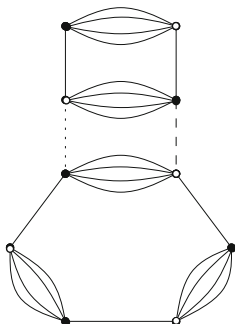
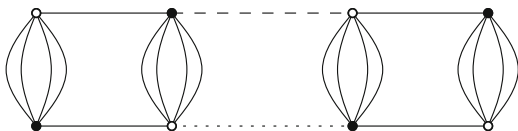
$$k\partial_k \lambda_3(k) = \frac{16\pi}{15}\lambda_1(k)\lambda_3(k)\frac{\eta(k) + 5}{[Z(k)k^2 + m^2(k)]^3}k^5. \tag{3.15}$$

$$k\partial_k \lambda_2(k) = \frac{24\pi}{15}\lambda_1(k)\lambda_2(k)\frac{\eta(k) + 5}{[Z(k)k^2 + m^2(k)]^3}k^5 - \frac{12\pi}{15}\lambda_1^3(k)\frac{\eta(k) + 5}{[Z(k)k^2 + m^2(k)]^4}k^5. \tag{3.16}$$

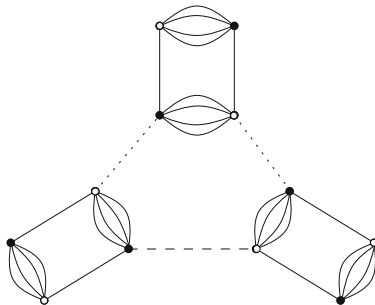
Taking into account the canonical dimension the renormalized dimensionless couplings are defined as:

$$m(k) = \sqrt{Z(k)}k\bar{m} \quad \lambda_1 = Z^2 k\bar{\lambda}_1(k)$$

**Fig. 2** Contribution to the 4-point interaction involved two vertices



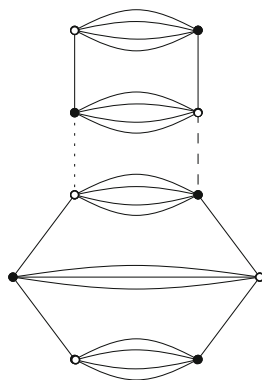
a



b

**Fig. 3** Contributions to the flow of  $\lambda_2$

**Fig. 4** Contribution to the flow of  $\lambda_3$



$$\lambda_2(k) = Z^3(k)\bar{\lambda}_2(k) \quad \lambda_3(k) = Z^3(k)\bar{\lambda}_3(k) \tag{3.17}$$

Using the flow equations (3.13), (3.12), (3.14), (3.16), and (3.15), we find for the dimensionless renormalized couplings the following autonomous system:

$$\eta(k) = \frac{5\pi}{2}\bar{\lambda}_1(k)\frac{1}{[1 + \bar{m}^2(k)]^2 - \bar{\lambda}_1(k)\frac{5}{6}\pi} \tag{3.18}$$

$$\beta_{m^2} = -(2 + \eta)\bar{m}^2(k) - \frac{4\pi}{3}\bar{\lambda}_1(k)\frac{\eta(k) + 5}{[1 + \bar{m}^2(k)]^2} \tag{3.19}$$

$$\beta_{\lambda_1} = -(1 + 2\eta)\bar{\lambda}_1(k) - (\bar{\lambda}_2 + 4\bar{\lambda}_3)\frac{4\pi}{15}\frac{\eta(k) + 5}{[1 + \bar{m}^2(k)]^2} + \bar{\lambda}_1^2(k)\frac{4\pi}{15}\frac{\eta(k) + 5}{[1 + \bar{m}^2(k)]^3} \quad (3.20)$$

$$\beta_{\lambda_3} = -3\eta\bar{\lambda}_3(k) + \frac{16\pi}{15}\bar{\lambda}_1\bar{\lambda}_3\frac{\eta(k) + 5}{[1 + \bar{m}^2(k)]^3}. \quad (3.21)$$

$$\beta_{\lambda_2} = -3\eta\bar{\lambda}_2(k) + \frac{24\pi}{15}\bar{\lambda}_1\bar{\lambda}_2\frac{\eta(k) + 5}{[1 + \bar{m}^2(k)]^3} - \bar{\lambda}_1^3\frac{12\pi}{15}\frac{\eta(k) + 5}{[1 + \bar{m}^2(k)]^4}, \quad (3.22)$$

with the definition:  $\beta_\sigma := k\partial_k\bar{\sigma}$ ,  $\sigma \in \{m^2, \lambda_1, \lambda_2, \lambda_3\}$ .

## 4 Fixed Points in the UV Regime

At vanishing  $\beta$ -functions we obtain the fixed points. In the neighborhood of these fixed points, the stability is determined by the linearized system of  $\beta$ -functions. All these points are studied in detail in this section.

### 4.1 Vicinity of the Gaussian Fixed Point

The autonomous system describing the flow of the dimensionless couplings admits a trivial fixed point for the values  $\bar{\lambda}_1 = \bar{\lambda}_2 = \bar{\lambda}_3 = \bar{m} = 0$  called Gaussian fixed point (GFP). Expanding our equations around this point, we find the reduced autonomous system:

$$\left\{ \begin{array}{l} \beta_{m^2} \approx -2\bar{m}^2 - \frac{20\pi\bar{\lambda}_1}{3}, \\ \beta_{\lambda_1} \approx -\bar{\lambda}_1 - \frac{4\pi}{3}(\bar{\lambda}_2 + 4\bar{\lambda}_3)\left(1 + \frac{\pi}{2}\bar{\lambda}_1 + 2\bar{m}^2\right) - \frac{11\pi}{3}\bar{\lambda}_1^2, \\ \beta_{\lambda_2} \approx \frac{\pi}{2}\bar{\lambda}_1\bar{\lambda}_2, \\ \beta_{\lambda_3} \approx -\frac{13\pi}{6}\bar{\lambda}_1\bar{\lambda}_3 \end{array} \right. \quad (4.1)$$

and the anomalous dimension:

$$\eta(k) \approx \frac{5\pi\bar{\lambda}_1}{2}. \quad (4.2)$$

These equations give the qualitative behavior of the RG trajectories around the GFP. In order to study its stability, we compute the *stability matrix*  $\beta_{ij} := \partial_i\beta_j$   $i \in \{m^2, \lambda_1, \lambda_2, \lambda_3\}$ , and evaluate each coefficient at the GFP. We find:

$$\beta_{ij}^{GFP} := \begin{pmatrix} -2 & 0 & 0 & 0 \\ -\frac{20\pi}{3} & -1 & 0 & 0 \\ 0 & -\frac{4\pi}{3} & 0 & 0 \\ 0 & -\frac{16\pi}{3} & 0 & 0 \end{pmatrix}, \tag{4.3}$$

with eigenvalues  $(-2, -1, 0, 0)$  and eigenvectors  $e_1^{GFP} = (\frac{9}{160\pi^2}, \frac{3}{8\pi}, \frac{1}{4}, 1)$ ;  $e_2^{GFP} = (0, \frac{3}{16\pi}, \frac{1}{4}, 1)$ ;  $e_3^{GFP} = (0, 0, 0, 1)$ ;  $e_4^{GFP} = (0, 0, 1, 0)$ . One recall that the *critical exponents* are the opposite values of the eigenvalues of the  $\beta_{ij}$ , and that the fixed point can be classified following the sign of their critical exponents. Hence, we have two relevant directions in the UV, with critical exponents 2 and 1, and two marginal couplings with zero critical exponents. Moreover, note that the critical exponents are equal to the canonical dimension around the GFP. Finally, note that the previous system of equations admits other fixed points, or a line of fixed points  $\bar{\lambda}_1 = \bar{m} = 0$ ;  $\bar{\lambda}_3 = -\bar{\lambda}_2/4$ , in addition to the Gaussian one. The same phenomenon happens away from the Gaussian fixed point. We will discuss this property in the next section.

For the moment, we are in a position to discuss the qualitative flow diagram around the Gaussian fixed point. First of all, note that all the coefficients of the  $\beta$ -function of the system (4.1) (i.e., the coefficients in the right-hand side of the system) are not negative. This fact seems to be a special feature of this model, meaning that the weight of the anomalous dimension does not dominate the vertex contribution. This fact is a first difference with respect to the similar non-Abelian  $\phi^6$  model studied in [14]. However, the analysis provided in this reference remains true, and the model is not asymptotically free. We will not repeat the complete analysis given in [14], but a qualitative argument is the following. Exploiting the fact that the hyperplans  $\bar{\lambda}_2 = 0$  and  $\bar{\lambda}_3 = 0$  are invariant under the flow, we can look at only a two-dimensional reduction of the complete system (4.1). We choose  $\bar{\lambda}_2 = 0$ , and plot the numerical integration of the reduced flow equation in Fig. 5 (on the left) below. In the domain,  $\bar{\lambda}_3 > 0$ , even if a given trajectory approaches of the Gaussian fixed point,  $\bar{\lambda}_1$  reaches a negative value, and it is ultimately repelled for  $k$  sufficiently large. The same phenomenon occurs for  $\bar{\lambda}_2$  in the plan  $\bar{\lambda}_2 < 0$  (see Fig. 5 on the right). We will give additional precision about the issue of the asymptotic freedom and/or safety in the next section.

### 4.2 Non-Gaussian Fixed Points

Solving numerically the systems (3.12)–(3.15), we find some non-Gaussian fixed points, whose relevant characteristics are summarized in Table 2. In addition to the Gaussian one, the system admits a line of fixed points, *LFP*:

$$LFP = \{\bar{m}^2 = 0, \bar{\lambda}_1 = 0, \bar{\lambda}_2 = -4\bar{\lambda}_3\}, \tag{4.4}$$

**Table 2** Summary of the properties of the non-Gaussian fixed points

FP	$\bar{m}^2$	$\bar{\lambda}_1$	$\bar{\lambda}_2$	$\bar{\lambda}_3$	$\eta$	$\theta^{(1)}$	$\theta^{(2)}$	$\theta^{(3)}$	$\theta^{(4)}$
$FP_1$	-0.3	0.005	0.0009	-0.0002	-6.3	-299	56.1	-11.7	5.8
$FP_2$	-0.7	0.008	0.0006	-0.0002	0.76	$-7.4 - 1.9i$	$-7.4 + 1.9i$	3.34	-0.12
$FP_3$	-0.9	0.0007	$3.32 \cdot 10^{-6}$	0.	1.3	-66.7	-42.63	-27.7	1.80
$FP_4$	-0.8	0.04	-0.02	0.	-5.9	-144.8	-14.4	-7.5	-5.4
$FP_5$	0.06	-0.006	0.002	0.	-0.04	1.9	1.09	-0.04	-0.01
$FP_6$	1.32	-0.5	-0.06	0.	-0.6	3.0	-1.23	-1.13	-0.39

Again, the critical exponents  $\theta^i$  are the opposite values of the eigenvalues of the stability matrix:  $\beta_* =: \text{diag}(-\theta_*^1, -\theta_*^2, -\theta_*^3, -\theta_*^4)$

with critical exponents:

$$\begin{cases} \theta^{(1)} &= -2, \\ \theta^{(2)} &= 0, \\ \theta^{(3)} &= -\frac{1}{2} \left( 1 + \sqrt{1 - \frac{128}{9} \pi^2 \bar{\lambda}_2} \right), \\ \beta_{\lambda_3} &= -\frac{1}{2} \left( 1 - \sqrt{1 - \frac{128}{9} \pi^2 \bar{\lambda}_2} \right). \end{cases} \tag{4.5}$$

The denominator of  $\eta$ ,  $D := [1 + \bar{m}^2(k)]^2 - \bar{\lambda}_1(k) \frac{5}{6} \pi$  introduces a singularity in the flow. At the Gaussian fixed point, and in a sufficiently small domain around, we have  $D > 0$ . But further away from the GFP,  $D$  may cancel, creating in the  $(\bar{\lambda}_1, \bar{m}^2)$ -plan a singularity line. The area below this line where  $D < 0$  is thus disconnected from the region  $D > 0$  connected to GFP. Then, we ignore for our purpose the fixed points in the disconnected region, for which  $D < 0$ . A direct computation shows that only the fixed points  $FP_2, FP_3, FP_5$ , and  $FP_6$  are relevant for an analysis in the domain connected to the Gaussian fixed point.

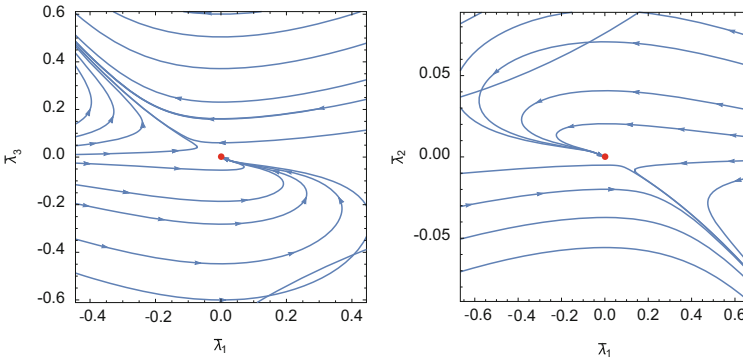
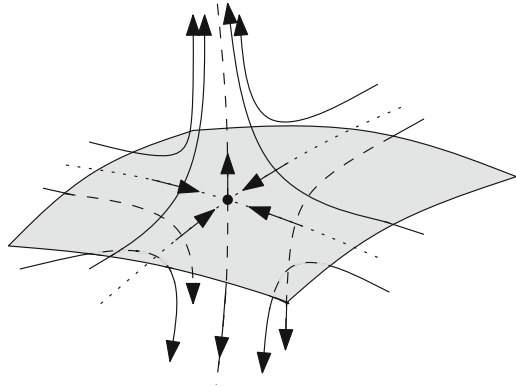


**Fig. 5** Phase portrait in the plans  $(\bar{\lambda}_1, \bar{\lambda}_3)$  for  $\bar{\lambda}_2 = 0$  (on the left) and in the plan  $(\bar{\lambda}_1, \bar{\lambda}_2)$ , for  $\bar{\lambda}_3 = 0$

**Fig. 6** Qualitative behavior of the RG trajectories around an IR fixed point. The critical surface is spanned by the relevant directions in the IR, and the arrows are oriented toward the IR direction. This illustrates the scenario of asymptotically safety



- The fixed points  $FP_2$  and  $FP_3$  are very similar. They have three irrelevant directions and one relevant direction in the UV. For each of these fixed points, the three irrelevant directions span a three-dimensional manifold on which trajectories run toward the fixed points in the IR, while the trajectories outside are repelled of this critical surface, as pictured in Fig. 6. This picture, the existence of a separatrix between two regions of the phase space is reminiscent of a critical behavior, with phase transition between a broken and a symmetric phase, and these separatrix are *IR-critical surfaces*. This interpretation is highlighted for the two fixed points in the zero momentum limit. Indeed, in both cases, the contributions in the effective action of the terms proportional to  $\bar{\lambda}_2$  and  $\bar{\lambda}_3$  can be neglected in comparison with the contributions to the first approximation of Ginsburg-Landau equation for  $\phi^4$  scalar complex theory. Note that for  $FP_2$  two critical exponents are complex, providing some oscillations of the trajectories, and implying that the fixed point is an IR-attractor in the two-dimensional manifold spanned by the eigenvectors corresponding to these two critical exponents. Moreover, the fixed point  $FP_6$  appears to be an IR fixed point, with coordinates of opposite sign.
- The fixed point  $FP_5$  has two relevant and two irrelevant directions in the UV. The relevant directions in the UV span a two-dimensional manifold corresponding to a *UV-multicritical surface* [32]. Such a surface is interesting for the UV-completion of the theory. Indeed, all the trajectories in the surface are oriented toward the fixed point in the UV, while the dimension of the surface gives an interesting number of physical parameter, providing an evidence in favor of the *asymptotic safety*.
- Finally, we have the line of fixed point, for which we will distinguish four cases:
  1. In the domain  $d_1 = \{\bar{\lambda}_2 < 0\}$  we have two relevant, one marginal and one irrelevant directions.
  2. At the point  $d_2 = \{\bar{\lambda}_2 = 0\}$ , we recover the GFP, with two relevant and two marginal directions.

3. In the domain  $d_3 = \{\bar{\lambda}_2 \in ]0, (\frac{3}{8\pi})^2\}$  we have three relevant and one marginal directions. One more time, this section of the critical line is interesting in view of the UV-completion of the theory and provides a supplementary evidence in favor of asymptotic safety. Indeed, in each point, the relevant directions in the UV span a three-dimensional UV-critical surface, in favor of the existence of a nontrivial asymptotically safe theory with three independent physical parameters. This line of fixed point has been recently discussed in [26] for a similar model improved by unconnected interaction bubbles.
4. In the domain  $d_4 = \{\bar{\lambda}_2 > (\frac{3}{8\pi})^2\}$ , the situation is very reminiscent of the previous one. We have three eigenvalues with negative real part and one equal to zero. Hence, we have three relevant and one marginal directions. The only difference in comparison with the domain  $d_3$  is that the eigenvalue has non-zero imaginary parts, giving some oscillations and attractor phenomena in the trajectories.

Finally, we briefly discuss the values of the anomalous dimensions. With our conventions, the couplings of the relevant operator are suppressed as a power of  $k$  in the UV limit  $k \rightarrow \infty$ . The couplings decrease when the trajectory goes away from the UV regime. However, the power law behavior is limited to the attractive region of the fixed point, far from its scaling regime it can deviate from the power law one. And we can evaluate this deviation. For instance, in the vicinity of  $FP_5$ , one deduce from (3.8) that the canonical dimension becomes:

$$[t_b]_{FP_5} \approx 3 - 1.6 \frac{N_b}{2}, \quad (4.6)$$

from which we deduce that all the interactions of valence up or equal to four become inessentials. The same phenomenon occurs in the vicinity of  $FP_4$ , where all the interactions up to these of valence four become irrelevant/relevant (according to their convention or inessential/essential). On the contrary, at the fixed points  $FP_2$  and  $FP_4$  the anomalous dimension is positive, meaning that the power counting is improved with respect to the Gaussian one, and irrelevant operators are enhanced in the UV.

## 5 Concluding Remarks

In this work we have studied the functional renormalization group applied to a U(1) tensor model. The flow equations of the coupling constants and mass parameter are deduced. The nontrivial behavior around the fixed point is also given. We have compelling evidence that the model studied in this paper is asymptotically safe in the UV regime. Let us remark that it is possible to extend the truncation to higher orders. Also, over regulators maybe tested. In this case the convergence of the fixed points can be studied order by order. For more detail, see [24] and [25].

**Acknowledgements** D.O.S research at the Max-Planck Institute is supported by the Alexander von Humboldt foundation.

## References

1. V. Rivasseau, The tensor track, III. Fortsch. Phys. **62**, 81 (2014). <https://doi.org/10.1002/prop.201300032> [arXiv:1311.1461 [hep-th]]
2. V. Rivasseau, The tensor track: an update. arXiv:1209.5284 [hep-th]
3. R. Gurau, J.P. Ryan, Colored tensor models - a review. SIGMA **8**, 020 (2012). <https://doi.org/10.3842/SIGMA.2012.020> [arXiv:1109.4812 [hep-th]]
4. R. Gurau, Colored group field theory. Commun. Math. Phys. **304**, 69 (2011). <https://doi.org/10.1007/s00220-011-1226-9> [arXiv:0907.2582 [hep-th]]
5. V. Rivasseau, Random Tensors and Quantum Gravity. arXiv:1603.07278 [math-ph]
6. D. Benedetti, R. Gurau, Symmetry breaking in tensor models. Phys. Rev. D **92**(10), 104041 (2015). <https://doi.org/10.1103/PhysRevD.92.104041> [arXiv:1506.08542 [hep-th]]
7. R. Gurau, The complete  $1/N$  expansion of colored tensor models in arbitrary dimension. Ann. Henri Poincaré **13**, 399 (2012). <https://doi.org/10.1007/s00023-011-0118-z> [arXiv:1102.5759 [gr-qc]]
8. R. Gurau, The  $1/N$  expansion of colored tensor models. Ann. Henri Poincaré **12**, 829 (2011). <https://doi.org/10.1007/s00023-011-0101-8> [arXiv:1011.2726 [gr-qc]]
9. D. Oriti, J.P. Ryan, J. Thurigen, Group field theories for all loop quantum gravity. New J. Phys. **17**(2), 023042 (2015). <https://doi.org/10.1088/1367-2630/17/2/023042> [arXiv:1409.3150 [gr-qc]]
10. D. Oriti, A quantum field theory of simplicial geometry and the emergence of spacetime. J. Phys. Conf. Ser. **67**, 012052 (2007). <https://doi.org/10.1088/1742-6596/67/1/012052> [hep-th/0612301]
11. C. Rovelli, Zakopane lectures on loop gravity. PoS QGQGS **2011**, 003 (2011). [arXiv:1102.3660 [gr-qc]]
12. C. Rovelli, Loop quantum gravity: the first twenty five years. Class. Quant. Grav. **28**, 153002 (2011). <https://doi.org/10.1088/0264-9381/28/15/153002> [arXiv:1012.4707 [gr-qc]]
13. S. Carrozza, D. Oriti, V. Rivasseau, Renormalization of tensorial group field theories: Abelian  $U(1)$  models in four dimensions. Commun. Math. Phys. **327**, 603 (2014). <https://doi.org/10.1007/s00220-014-1954-8> [arXiv:1207.6734 [hep-th]]
14. S. Carrozza, Ann. Inst. Henri Poincaré Comb. Phys. Interact. **2**, 49–112 (2015). <https://doi.org/10.4171/AIHPD/15> [arXiv:1407.4615 [hep-th]]
15. D. Ousmane Samary, F. Vignes-Tourneret, Just renormalizable TGFT's on  $U(1)^d$  with gauge invariance. Commun. Math. Phys. **329**, 545 (2014). <https://doi.org/10.1007/s00220-014-1930-3> [arXiv:1211.2618 [hep-th]]
16. J. Ben Geloun, V. Rivasseau, A renormalizable 4-dimensional tensor field theory. Commun. Math. Phys. **318**, 69 (2013). <https://doi.org/10.1007/s00220-012-1549-1> [arXiv:1111.4997 [hep-th]]
17. J. Ben Geloun, D. Ousmane Samary, 3D tensor field theory: renormalization and one-loop  $\beta$ -functions. Ann. Henri Poincaré **14**, 1599 (2013). <https://doi.org/10.1007/s00023-012-0225-5> [arXiv:1201.0176 [hep-th]]
18. J. Ben Geloun, Two and four-loop  $\beta$ -functions of rank 4 renormalizable tensor field theories. Class. Quant. Grav. **29**, 235011 (2012). <https://doi.org/10.1088/0264-9381/29/23/235011> [arXiv:1205.5513 [hep-th]]
19. D. Ousmane Samary, Beta functions of  $U(1)^d$  gauge invariant just renormalizable tensor models. Phys. Rev. D **88**(10), 105003 (2013). <https://doi.org/10.1103/PhysRevD.88.105003> [arXiv:1303.7256 [hep-th]]

20. J.B. Geloun, R. Martini, D. Oriti, Functional renormalisation group analysis of tensorial group field theories on  $\mathbb{R}^d$ . arXiv:1601.08211 [hep-th]
21. J.B. Geloun, R. Martini, D. Oriti, Functional renormalization group analysis of a tensorial group field theory on  $\mathbb{R}^3$ . *Europhys. Lett.* **112**(3), 31001 (2015). <https://doi.org/10.1209/0295-5075/112/31001> [arXiv:1508.01855 [hep-th]]
22. D. Benedetti, V. Lahoche, Functional renormalization group approach for tensorial group field theory: a Rank-6 model with closure constraint. arXiv:1508.06384 [hep-th]
23. D. Benedetti, J. Ben Geloun, D. Oriti, Functional renormalisation group approach for tensorial group field theory: a rank-3 model. *JHEP* **1503**, 084 (2015). [https://doi.org/10.1007/JHEP03\(2015\)084](https://doi.org/10.1007/JHEP03(2015)084) [arXiv:1411.3180 [hep-th]]
24. V. Lahoche, D. Ousmane Samary, Functional renormalization group for the  $U(1)$ - $T_6^6$  tensorial group field theory with closure constraint. *Phys. Rev. D* **95**(4), 045013 (2017). <https://doi.org/10.1103/PhysRevD.95.045013> [arXiv:1608.00379 [hep-th]]
25. S. Carrozza, V. Lahoche, Asymptotic safety in three-dimensional  $SU(2)$  group field theory: evidence in the local potential approximation. *Class. Quant. Grav.* **34**(11), 115004 (2017). <https://doi.org/10.1088/1361-6382/aa6d90> [arXiv:1612.02452 [hep-th]]
26. J.B. Geloun, T.A. Koslowski, Nontrivial UV behavior of rank-4 tensor field models for quantum gravity. arXiv:1606.04044 [gr-qc]
27. P. Donà, A. Eichhorn, P. Labus, R. Percacci, Asymptotic safety in an interacting system of gravity and scalar matter. *Phys. Rev. D* **93**(4), 044049 (2016). <https://doi.org/10.1103/PhysRevD.93.044049> [arXiv:1512.01589 [gr-qc]]
28. P. Donà, A. Eichhorn, R. Percacci, Consistency of matter models with asymptotically safe quantum gravity. *Can. J. Phys.* **93**(9), 988 (2015). <https://doi.org/10.1139/cjp-2014-0574> [arXiv:1410.4411 [gr-qc]]
29. A. Eichhorn, T. Koslowski, Continuum limit in matrix models for quantum gravity from the functional renormalization group. *Phys. Rev. D* **88**, 084016 (2013). <https://doi.org/10.1103/PhysRevD.88.084016> [arXiv:1309.1690 [gr-qc]]
30. C. Wetterich, Average action and the renormalization group equations. *Nucl. Phys. B* **352**, 529 (1991). [https://doi.org/10.1016/0550-3213\(91\)90099-J](https://doi.org/10.1016/0550-3213(91)90099-J)
31. D.F. Litim, Optimization of the exact renormalization group. *Phys. Lett. B* **486**, 92 (2000). [https://doi.org/10.1016/S0370-2693\(00\)00748-6](https://doi.org/10.1016/S0370-2693(00)00748-6) [hep-th/0005245]
32. R. Percacci, Asymptotic Safety (2008). arXiv: 0709.3851, [hep-th]